

Supplementary Materials

Nanobody Detection of Standard Fluorescent Proteins Enables Multi-Target DNA-PAINT with High Resolution and Minimal Displacement Errors

Shama Sograte-Idrissi^{1,2,4,†}, Nazar Oleksiievets^{3,†}, Sebastian Isbaner³, Mariana Eggert-Martinez^{1,2,4}, Jörg Enderlein³, Roman Tsukanov^{3,*}, Felipe Opazo^{1,2,*}

¹Institute of Neuro- and Sensory Physiology, University Medical Center Göttingen, 37073 Göttingen, Germany

²Center for Biostructural Imaging of Neurodegeneration (BIN), University of Göttingen Medical Center, 37075 Göttingen, Germany

³Third Institute of Physics – Biophysics, Georg August University, 37077 Göttingen, Germany

⁴International Max Planck Research School for Molecular Biology, Göttingen, Germany

[†]These authors contribute equality to this work

*Corresponding authors: fopazo@gwdg.de, roman.tsukanov@phys.uni-goettingen.de

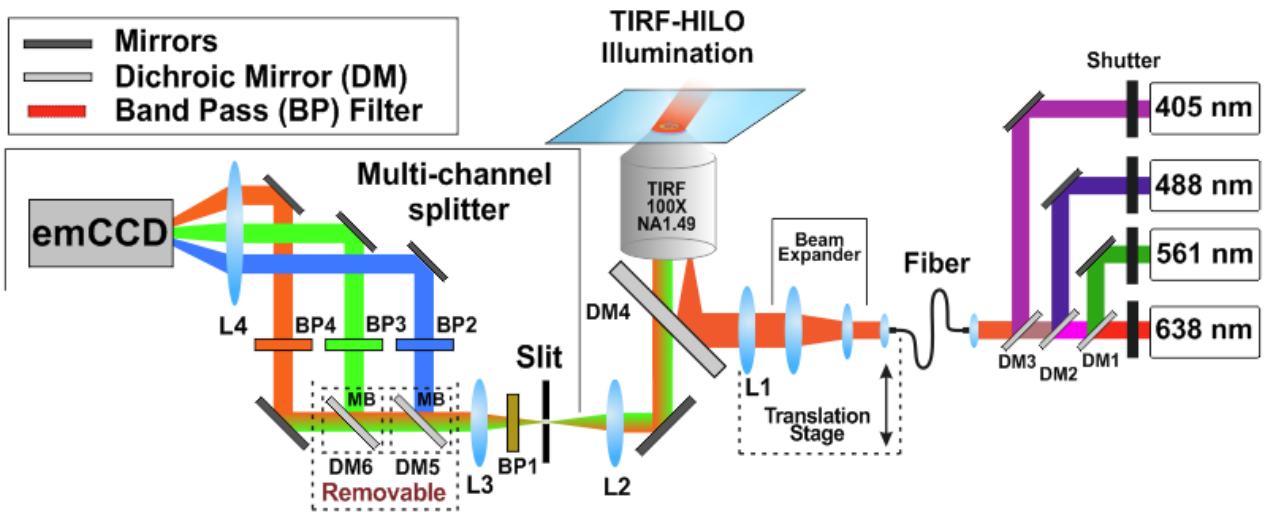
Running title: Multicolor DNA-PAINT using nanobodies

Keywords: Nanobodies, Super-resolution microscopy, multi-color imaging, TIRF, microfluidics, DNA-PAINT, molecular localization, sdAb, GFP, mCherry, mtagBFP, multiplexing

1 **Custom-built optical setup description**

2 Measurements were performed on an in-house-built optical setup. In brief, the excitation part
3 included four lasers: 405 nm (CUBE 405-100C, Coherent), 488 nm (PhoxX+ 488-100, Omicron),
4 561 nm (MGL-FN-561-100, Changchun), and 638 nm (PhoxX+ 638-150, Omicron). Manual shutters
5 were used to easily switch between excitation lasers. The lasers were combined into the same optical
6 path using dichroic mirrors DM1 (BrightLine DiO2-R561, Semrock), DM2 (BrightLine FF495-Di03,
7 Semrock), and DM3 (zt405 RDC, Chroma). Then, the laser beams were coupled into a single-mode
8 fiber (P1-460B-FC-2, Thorlabs) with typical coupling efficiency of 40-50%. After exiting the fiber,
9 the beam was collimated and expanded by a factor of 3.6X using telescopic lenses. In order to
10 achieve wide-field illumination, lens L1 (AC508-200-A-ML, Thorlabs) focused collimated laser
11 beam on the back focal plane of the high-NA objective (UAPON 100x oil, 1.49 NA, Olympus). In
12 order to switch between Epi-, HILO-, or TIRF-illumination schemes, the translation stage TS
13 (LNR50M, Thorlabs) was used to mechanically shift the corresponding optical elements. The
14 translation XY stage (M-406, Newport) ensured smooth and stable sample movement during the
15 scan.

16 A separate translation stage with a differential micrometer screw (DRV3, Thorlabs) was holding the
17 objective and was used for focusing. The emitted fluorescence was separated from the excitation
18 laser using the multi-band dichroic mirror DM4 (Di03 R405/488/532/635, Semrock). Lens L2
19 (AC254-200-A-ML, Thorlabs) was used as a tube lens. An adjustable slit (SP60, OWIS) was
20 positioned in the image plane and was used to limit the field of view. The multi-band filter BP1
21 (ZET488/561/635m, Chroma) was used to filter out laser remains in the detection path. Lenses L3
22 (AC254-100-A, Thorlabs) and L4 (AC508-150-A-ML, Thorlabs) were used to transfer the image
23 plane from the slit to the EMCCD camera (iXon Ultra 897, Andor), thereby providing rectangular
24 space for wavelength-based splitting of the emission light into two or three emission channels
25 according to the experimental requirements. For this purpose, the dichroic mirrors DM5 (Chroma
26 550 LPXR) and DM6 (FF648-Di01, Semrock) were positioned on magnetic bases MB (KB50/M,
27 Thorlabs). For each channel, additional band-pass filters were used: BP2 (BrightLine FF 445/20,
28 Semrock) for the blue channel, BP3 (BrightLine FF 536/40, Semrock) for the green channel, and
29 BP4 (BrightLine HC 692/40, Semrock) for the red channel. The overall magnification factor of the
30 optical setup was 166.6X, the pixel size was 103.5 nm x 103.5 nm and the full field of view was 53
31 μm X 53 μm . Focus stability was achieved by robust construction of the custom microscope body,
32 tightly fixing the 8-well chamber (155411PK, ThermoFisher Scientific) to the sample holder and
33 keeping the temperature in the room stable.



1

2 **Figure S1. Schematic drawing of custom wide-field TIRF optical setup.** The excitation is equipped with four lasers
 3 and allows excitation of fluorophores on broad spectral range. Multi-channel detection enables simultaneous imaging of
 4 fluorophores with different emission spectrum on the same CCD camera. Number of emission channels can be easily
 5 switched between one, two and three channels by removing the dichroic mirrors DM5 or/and DM6. The size of region of
 6 interest is controlled by a slit.

7

8

9

10

11

12

13

14

15

16

17

18

19

20

21

22

1 **Localization accuracy and resolution estimations**

2 Detailed numbers as for each reconstructed image resolution are listed in the Table S1.

Cell name	Organelle, protein, docking	NeNa, nm	FRC, nm	Cell name	Organelle, protein, docking	NeNa, nm	FRC, nm
Fig 4, C1	Mito GFP P1*	20	21	Fig 4, D1	Mito RFP P2*	19	22
	Golgi RFP P2*	18	27		Golgi GFP P1*	18	24
	Nucleus BFP P3*	22	32		Nucleus BFP P3*	23	38
Fig 4, C2	Mito GFP P1*	22	34	Fig 4, D2	Mito RFP P2*	20	28
	Golgi RFP P2*	16	23		Golgi GFP P1*	19	20
	Nucleus BFP P3*	23	34		Nucleus BFP P3*	19	24
				Fig 4, D3	Mito RFP P2*	14	24
			Golgi GFP P1*		18	27	
			Nucleus BFP P3*		17	26	

3 **Table S1. Average localization precision (NeNa) and resolution estimation using FRC technique for each of the**
 4 **reconstructed images presented in Figure 4. Cell names appear according to the order in Figure 4.**

5

6

7

8

9

10

11

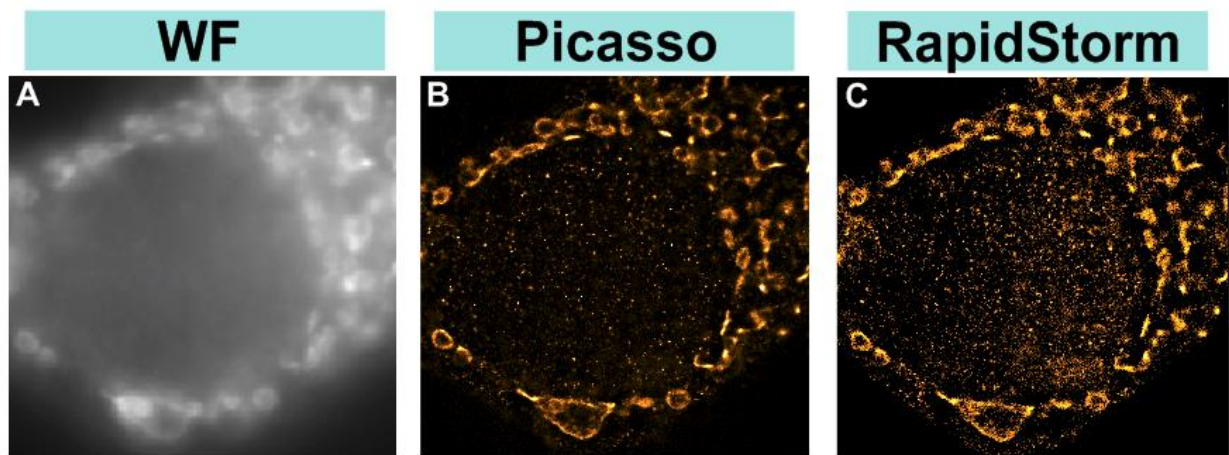
12

13

14

1 **DNA-PAINT analysis toolkits comparison: Picasso vs. Rapidstorm**

2 Verification of Picasso analysis was done by analysing same image with RapidStorm.¹ Recorded
3 DNA-PAINT movie was loaded into RapidStorm. Blinking event were identified by setting the
4 intensity threshold to 60 % of a total brightness. Resolution (both X and Y direction) was set to 10
5 nm/pixel. The comparison between reconstructed images shown on Figure S2. The achieved
6 resolution was estimating by exporting the localization file output and then running it into
7 SQUIRREL ImageJ plugin². Resulting numbers and comparison to Picasso output shown on Table
8 S1. We saw good agreement Picasso and RapidStorm results.



10 **Figure S2. Comparison between Picasso and RapidStorm software packages.** (A) Wide-field (WF) diffraction-
11 limited image of GFP protein. (B) Reconstructed super-resolution image obtained with Picasso software. (C)
12 Reconstructed super-resolution image obtained with Picasso software.

13

14

15

16

17

18

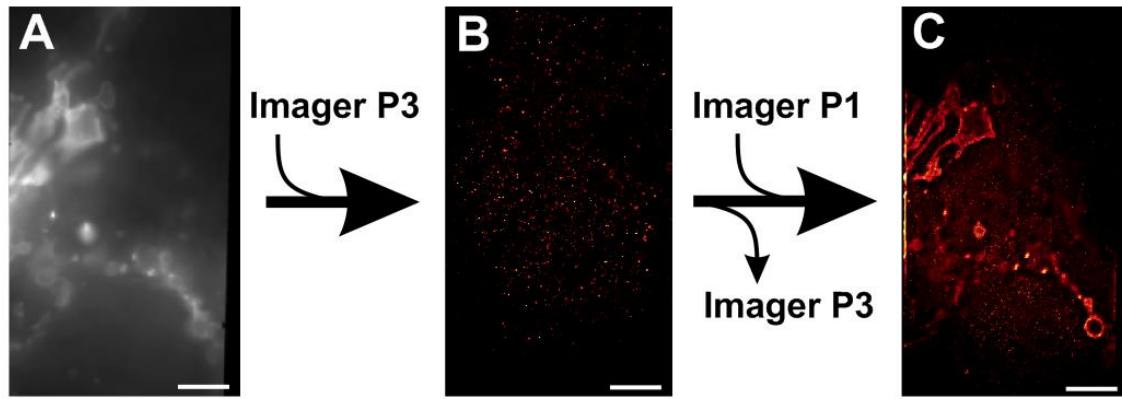
19

20

21

22

23



1

2 **Figure S3. Control experiment for the nanobody specificity and the stickiness of the imager strand inside fixed**
3 **COS7 cell transfected with TOM70-GFP-P1*.** (A) wide-field image of TOM70 GFP. (B) Super-resolution image from
4 a DNA-PAINT movie taken in presence of P3 imager. Only few random localization events detected in presence of the
5 imager P3 (C) Super-resolution image of the same region of interest, taken in presence of P1 imager (after
6 washing/removing the imager P3).

7

8

9

10

11

12

13

14

15

16

17

18

19

20

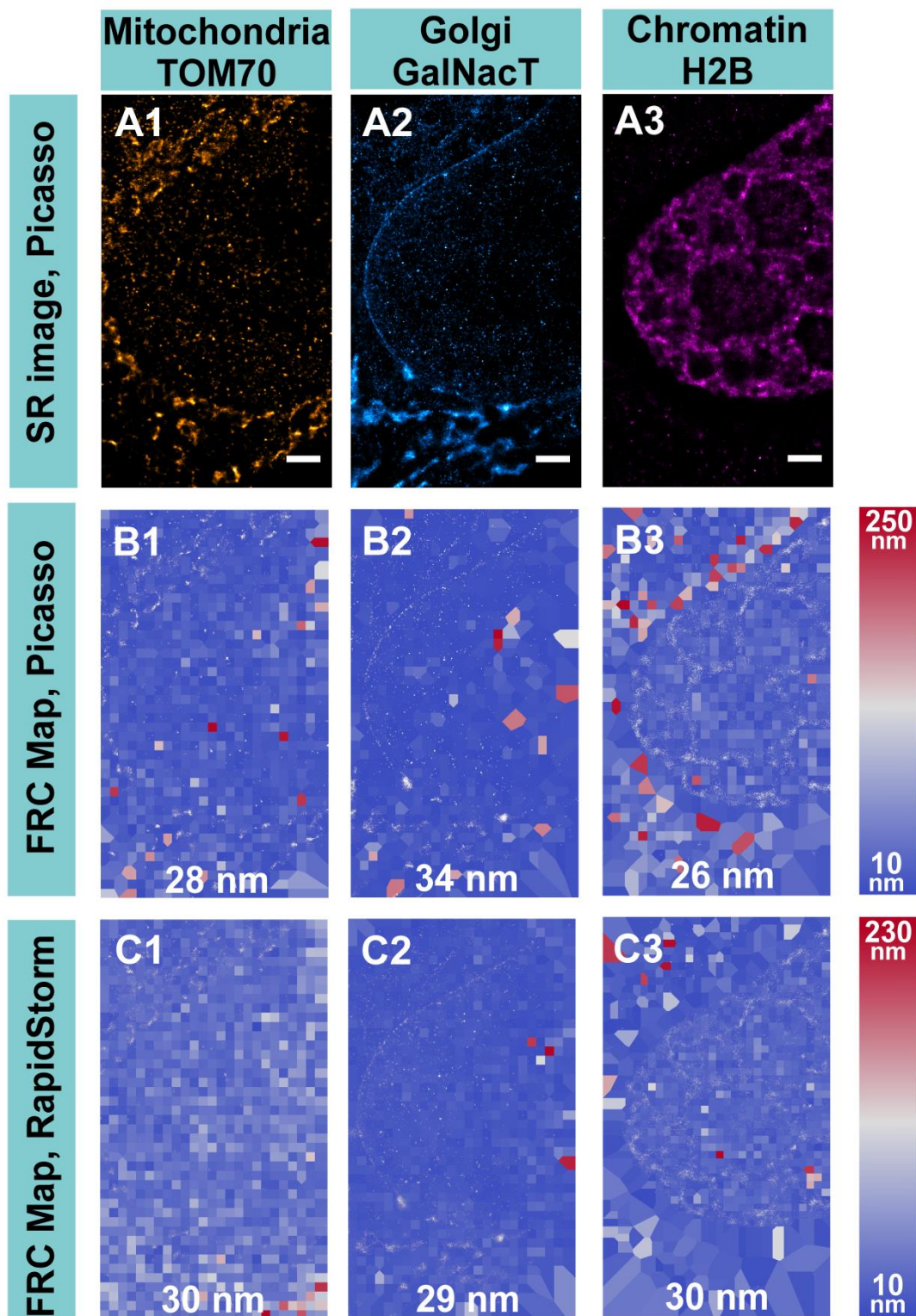
21

22

23

1 **DNA-PAINT Fourier Ring Correlation resolution maps**

2 For NanoJ-SQUIRREL analysis stack of two statistically independent super-resolution images of the
3 same structure were reconstructed using Picasso and RapidStorm software. Then using ‘Calculate
4 FRC Map’ feature (block per pixel value 25 and pixel size 10 nm) the FRC map was made and
5 overlaid with respective super-resolution image. Average FRC resolution value was obtained by
6 finding the mean value from the area with high localization density. For this purpose, obtained super-
7 resolution image was cropped and whole procedure was repeated for this area. The average
8 resolutions obtained are 26 nm for Picasso and 30 nm for RapidStorm.



1

2 **Figure S4. Resolution estimation using Fourier Ring Correlation maps realized by SQUIRREL ImageJ plugin².**
 3 Comparison between Picasso and RapidStorm analysis tools. (A1-3) Super-resolution DNA-PAINT images of COS7 cell
 4 organelles reconstructed by Picasso. (B1-3) FRC map overlaid with the corresponding super-resolution images, as
 5 reconstructed by Picasso toolkit. The color bar on the right-hand side encodes the FRC resolution. (C1-3) FRC map
 6 overlaid with the corresponding super-resolution images, as reconstructed by RapidStorm toolkit. The color bar on the
 7 right-hand side encodes the FRC resolution. The numbers on the bottom of the images (B1-3) and (C1-3) represent the
 8 FRC resolution averaged over the object region.

1 **Bibliography**

- 2 1. Wolter, S. *et al.* rapidSTORM: accurate, fast open-source software for localization
3 microscopy. *Nat. Methods* **9**, 1040–1041 (2012).
- 4 2. Culley, S. *et al.* Quantitative mapping and minimization of super-resolution optical imaging
5 artifacts. *Nat. Methods* **15**, 263–266 (2018).

6